IFAC-PapersOnLine, Volume 52, Issue 12, 2019, pp. 214-218
21st IFAC Symposium on Automatic Control in Aerospace ACA 2019: Cranfield, U.K, 27–30 August 2019
DOI: 10.1016/j.ifacol.2019.11.245

$\mathrm{H}_\infty/\mathrm{LQR}$ Optimal Control for a Supersonic Air-Breathing Missile of Asymmetric Configuration ⋆

Raymond Vin Vincent * **John Economou** * † **David Galvao Wall** *
John Cleminson **

* *Aero-mechanical Systems Group, Centre for Defence Engineering, Cranfield Defence & Security, Defence Academy of the United Kingdom, Shrivenham, SN6 8LA, UK*
† *j.t.economou@cranfield.ac.uk*
** *Defence Science and Technology Laboratory Portsdown West, Portsdown Hill Rd, Fareham, PO17 6AD, UK*

Abstract: Robust control is challenging to achieve for air-breathing missiles operating in a high Mach number regime, such as at high supersonic speeds ($M > 3$). The challenge arises because of strong couplings, significant non-linearities and large uncertainties in the aerodynamics and propulsion system. The feasibility of achieving robust control in such applications is strongly linked to the development of an appropriate control design structure. The purpose of this paper is to illustrate that in order to stabilise a highly unstable airframe and achieve the required performance, a hybrid of two control schemes may be used to achieve best results. A state feedback linear quadratic regulator is used to stabilise the plant and a forward path H_∞ optimal controller is used to achieve the required performance and robustness. We also highlight the complementary attributes of the two control schemes that together can generate a more robust controller; LQR is used since it can achieve good gain and phase margins, whereas, the H_∞ control method is better equipped to deal with uncertainties.

Keywords: Missile, H-Infinity, Linear Quadratic Regulator, LQR, Optimal Control, Asymmetric

NOMENCLATURE

Symbol	Description	Units
x, y, z	Cartesian body axes	m
v, w	Translational velocity	m/s
p, q, r	Rotational velocity about x, y, z axes, respectively	rad/s
U	Constant forward velocity	m/s
ξ, η, ζ	Aileron, Elevator and Rudder deflection	$radians$
α	Angle of attack	$radians$
β	Sideslip angle	$radians$
ϕ	Roll angle	$radians$
a_y, a_z	Accelerations along y and z axes, respectively	m/s^2
γ	Controller performance metric	−

1. INTRODUCTION

Classical single-input, single-output (SISO) design techniques known for their intuitive nature have been used in the development of missile autopilots for decades. However, as system complexities such as high non-linear missile characteristics and strong airframe/propulsion system couplings arise, it often becomes very cumbersome to design controllers using such methods. It is also well known that multiple-input, multiple-output (MIMO) systems are handled better with optimal multi-variable control methods. The Linear, Quadratic and Gaussian (LQG) (Anderson and Moore (1989)) with Linear Quadratic Regulators (LQR) is one such method. These techniques have been around since the 1960s and are widely used in academia and industry alike. LQG uses white noise to approximate the model uncertainties and disturbances to the system, which in practice may not be very meaningful and can even be too conservative at times. However, LQR (assuming all the states are available) provides an optimal controller with guaranteed stability and good phase and gain margins (Safonov and Athans (1976)). To account for the robustness, a H_∞ optimal controller (Zames (1981)) may be used as they can address both performance and robustness requirements in a single design metric, γ. H_∞ optimal control techniques have been successfully used in the development of missile and other air vehicle autopilots for several decades (Reichert (1990), Thompson and Chiang (1990), Hyde (1995), Reichert (1989), Urban et al. (1999)). Glover and Mcfarlane (1989) solves the problem of robust stability for linear systems with unstructured uncertainty.

Therefore, in this paper, we combine two control methods to capitalize on their strengths. First we describe the liner time-invariant state space model of the missile airframe. Then, we use a two loop control structure to design a LQR controller on the inner loop and a mixed-sensitivity H_∞ optimal controller on the outer loop. Autopilot transient responses and controller effort are then shown and discussed.

2. MISSILE DYNAMICS

The developed model is a 180° Bank-To-Turn (BTT) missile, as this form of steering aligns best with the incidence constraints of the air-breathing motor; and also BTT steering can help

⋆ This project is part-sponsored by the Defence Science and Technology Laboratory (DSTL) of the United Kingdom and the other part by Cranfield University.

keep aerodynamic cross-coupling (caused by the asymmetric configuration of the airframe) to a lower level than if the steering were skid-to-turn (STT). The linear airframe dynamics of the missile are described by the state space equations (1).

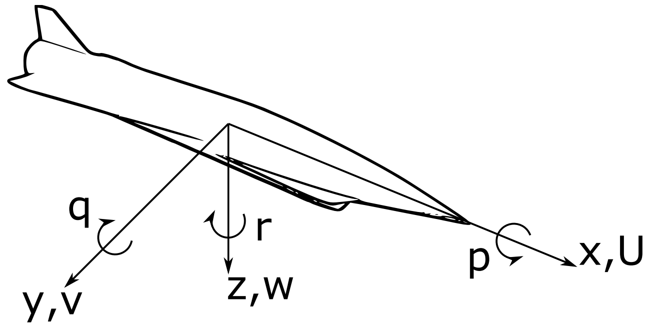

Fig. 1. Missile Airframe (with Body Axes superimposed)

$$\begin{aligned} \dot{x} &= Ax + Bu \\ y &= Cx + Du \end{aligned} \tag{1}$$

We ignore gravity and the state vector $\mathbf{x}$ is selected as $[p \quad q \quad r \quad w \quad v]'$, the control input vector $\mathbf{u}$ as $[\xi \quad \eta \quad \zeta]'$, the plant output vector $\mathbf{y}$ as $[p \quad q \quad r \quad a_y \quad a_z]'$ and the matrices $A_{5\times5}$, $B_{5\times3}$, $C_{5\times5}$ and $D_{5\times3}$ are as follows:

$$A = \begin{bmatrix} l_p & l_q & l_r & l_w & l_v \\ m_p & m_q & m_r & m_w & m_v \\ n_p & n_q & n_r & n_w & n_v \\ y_p + \alpha U & y_q & (y_r - U) & y_w & y_v \\ z_p - \beta U & (z_q + U) & z_r & z_w & z_v \end{bmatrix}$$

$$B = \begin{bmatrix} l_\xi & l_\eta & l_\zeta \\ m_\xi & m_\eta & m_\zeta \\ n_\xi & n_\eta & n_\zeta \\ y_\xi & y_\eta & y_\zeta \\ z_\xi & z_\eta & z_\zeta \end{bmatrix}$$

$$C = \begin{bmatrix} 1 & 0 & 0 & 0 & 0 \\ 0 & 1 & 0 & 0 & 0 \\ 0 & 0 & 1 & 0 & 0 \\ 0 & 0 & 0 & y_w & y_v \\ 0 & 0 & 0 & z_w & z_v \end{bmatrix}$$

$$D = \begin{bmatrix} 0 & 0 & 0 \\ 0 & 0 & 0 \\ 0 & 0 & 0 \\ y_\xi & y_\eta & y_\zeta \\ z_\xi & z_\eta & z_\zeta \end{bmatrix}$$

l_i, m_i and n_i are partial derivatives of the roll, pitch and yaw aerodynamic angular accelerations with respect to the appropriate i about the respective axis. y_i and z_i are the partial derivatives of aerodynamic translational acceleration with respect to the appropriate i along the respective axis. U is the forward velocity and α is angle of attack and β the sideslip angle.

3. AUTOPILOT DESIGN

The outputs being controlled are the roll angle ϕ which is acquired by integrating the roll rate p, the acceleration in y-direction and z-direction, a_y and a_z, respectively.

The nature of the airframe happens to be inherently unstable. In our approach we first stabilise the airframe using LQR, which forms the inner closed loop system. Once stability is achieved with good margins, we then solve the optimisation problem by using the mixed-sensitivity optimal control method to get the desired tracking performance. LQR generates a static gain matrix K_s and this is ideal because we want to achieve robust stability without increasing the order of the inner-closed loop system. Figure (3) shows the isolated inner loop, which is equivalent to G_s in figure (5).

The mixed-sensitivity H_∞ optimal control method is chosen for performance because it has the framework to explicitly take uncertainties into account, which the traditional LQG method lacks (S. Skogestad (1988)). The reference tracking autopilot topology with the H_∞ controller in the forward path of the outer loop and a state-feedback LQR inner controller is shown in figure (2).

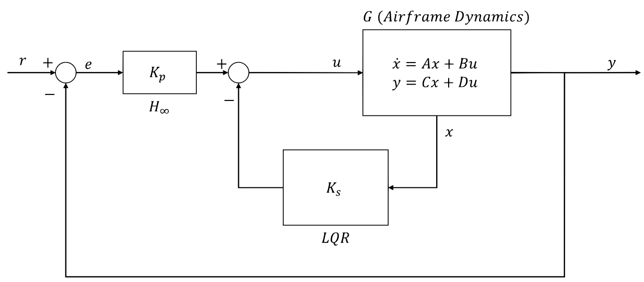

Fig. 2. Control Topology

3.1 *Linear Quadratic Regulator*

The LQR controller is generated by minimizing the cost function J shown in (2). Detailed derivations can be found in Zhou and Doyle (1998), Skogestad and Postlethwaite (1996). Proofs for stability are found in Safonov and Athans (1976) and Anderson and Moore (1989).

$$J = \int_0^\infty x(t)^T Q x(t) + u(t)^T R u(t) \quad dt \tag{2}$$

Q and R are both positive definite weighting matrices chosen by the designer. Therefore, the controller generated is optimal only to the chosen weights.

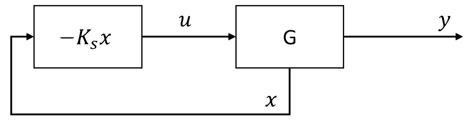

Fig. 3. LQR Regulator

The control law $u(t) = -K_s x(t)$, where,

$$K_s = R^{-1} B^T X \tag{3}$$

and $X = X^T \geq 0$ is the unique solution to the Ricatti equation (4). Doyle et al. (1989)

$$A^T X + XA - XBR^{-1}X + Q = 0 \tag{4}$$

It is known that for the dynamic system described in (1), given that (A, B) is stabilisable and (C, A) is detectable, then the solution X to the ricatti equation (4), which minimises the cost function (2) is always stable. (Doyle et al. (1989): *lemma 3* and Cimen (2008): *lemma 1*)

3.2 H_∞ *optimal control*

The H_∞ control optimization problem was developed by Zames (1981) and further work done by Doyle et al. (1989).

Unlike, LQR where the weighting matrices essentially apply a constant upper gain limit across the frequency response, the H_∞ optimal control method allows the designer to shape the frequency response with transfer functions, making it a somewhat less conservative and more tailored approach.

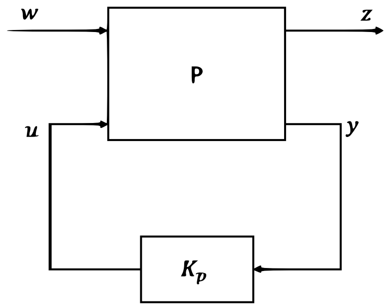

Fig. 4. The General Configuration

The system described by (1) with the control topology shown in figure (2) can be recast to the general control configuration (Figure 4), so that it complies with the H_∞ framework. Figure (4) is described by (5).

$$\begin{bmatrix} z \\ v \end{bmatrix} = P(s) \begin{bmatrix} w \\ u \end{bmatrix} = \begin{bmatrix} P_{11}(s) & P_{12}(s) \\ P_{21}(s) & P_{22}(s) \end{bmatrix} \begin{bmatrix} w \\ u \end{bmatrix} \tag{5}$$

$$u = K_p(s)v \tag{6}$$

Where, $P(s)$ is the state-space realisation of the generalised plant, which consists of the stable closed loop LQR plant $G_s(s)$ and the performance and control effort weights, $W_e(s)$ and $W_u(s)$, respectively. Topology of $P(s)$ is shown in figure (5).

"The H_∞ optimal control problem solves for all stabilising controllers $K_p(s)$ which minimises $\|F_l(P(s), K_p(s)\|_\infty$." (Zhou and Doyle (1998))

Solving for the optimal controller is numerically and theoretically complicated and the characteristics of optimal controllers are sometimes undesired (higher order). Therefore a sub-optimal solution can be sought after.

"Given $\gamma > 0$, find all admissible controllers $K_p(s)$, if there are any, such that $\|F_l(P, K_p)\|_\infty < \gamma$." (Zhou and Doyle (1998))

Detailed solution to the H_∞ optimal control problem can be found in Doyle et al. (1989) and further summaries in Skogestad and Postlethwaite (1996).

The design approach taken to solve the H_∞ norm of the plant is called the mixed-sensitivity optimal control.

$$\|F_l(P, K_p)\|_\infty = \left\| \begin{matrix} W_e S \\ W_u K_p S \end{matrix} \right\|_\infty < \gamma \tag{7}$$

Where, the sensitivity function $S = (1 + G_s K_p)^{-1}$, W_e is the performance weight and W_u the control weighting function.

W_e and W_u are both stable proper transfer functions.

$S(i\omega)$ is shaped as a high pass filter so that the low-frequency steady state error is minimised to get the desired tracking performance. Therefore, W_e is designed so that the inequality $\|W_e S\|_\infty \leq 1$ is met.

$K_p S(j\omega)$ is shaped to be a low pass filter to minimises the cost of the control effort and reject the high-frequency sensor noise. Therefore, W_u is designed so that the inequality $\|W_u K_p S\|_\infty \leq 1$ is met (Skogestad and Postlethwaite (1996)). Therefore, for a physically realisable solution, the design metric γ has to obey the inequality given in (8).

$$\gamma < 1 \tag{8}$$

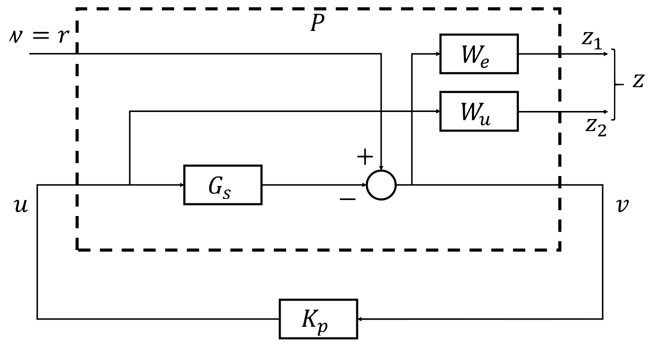

Fig. 5. Mixed-Sensitivity Optimisation Problem

4. RESULTS AND DISCUSSION

The weights Q, R, W_e and W_u were designed according to specification and guidelines given in Skogestad and Postlethwaite (1996) and Zhou and Doyle (1998).

$$\begin{aligned} Q &= \begin{bmatrix} 1 & 0 & 0 & 0 & 0 \\ 0 & 10 & 0 & 0 & 0 \\ 0 & 0 & 10 & 0 & 0 \\ 0 & 0 & 0 & 0.01 & 0 \\ 0 & 0 & 0 & 0 & 0.01 \end{bmatrix} \\ R &= I_{3\times3} \\ W_e(s) &= diag[\frac{s+10}{2s+0.1}, 0, 0, \frac{s+4}{2s+0.04}, \\ &\qquad \frac{s+4}{2s+0.04}] \\ W_u(s) &= \frac{s+0.009425}{0.0001s+94.25} I_{3\times3} \end{aligned} \tag{9}$$

Using the weights from (9), we achieve a γ of 0.7585. Figure (6) is the response to the plant described by (1) when the desired input pitch acceleration $a_z = 100\ m/s^2$ and figure (7) the corresponding controller effort. The plant is allowed the first 5 seconds to settle to 0 from any initial conditions the plant may be on due to trim conditions. For a step input at $t = 5s$ the missile reference tracks with a transient response under approximately 1 second with no over shoot and no steady-state error. An elevator fin deflection of $0.02\ rad$ is required to hold the acceleration at $100\ m/s^2$. There is also the expected non-minimum phase response that is characteristic of a rear-fin controlled missile. The missile airframe is highly coupled and this is evident in the responses of the other outputs. Roll angle ϕ has a displacement of up to $0.8\ rad$, which is expected for a high acceleration demand, it however settles back to 0. The roll and yaw body rates (p and r, respectively) are regulated, and the pitch rate (q) exhibits the expected steady-state offset for this manoeuvre. Aileron and rudder deflections show the missile counteracting the coupling effects of the missile.

The following results disregard the propulsion constraints that impose 180°BTT steering and we have assumed STT steering;

this is done only to illustrate the response of the hybrid controller to aerodynamic coupling. The response to a desired pure yaw acceleration step of 100 m/s^2 at $t = 5s$ is shown in figures (8) and (9). Characteristics of the response are somewhat similar to the pitch accelerations, but in the opposite direction. Since it is a non-axisymmetric missile, we see a steady-state fin deflection in both aileron and the rudder control to hold the yaw acceleration step demand.

Figures (10) and (11) are the responses when we demand a step of 100 m/s^2 at pitch and yaw accelerations (a_z and a_y respectively) simultaneously. The autopilot is able to meet both demands and the transient response times for a_z and a_y are still similar. The aileron fin angle reaches maximum deflection (i.e. saturation) briefly, but it still manages to regulate the roll angle ϕ to 0 rad. As expected, the elevator and rudder deflection angles are larger in amplitude than compared to those of the previous results but are within expected bounds ($+/-0.35$ rad).

5. CONCLUSION

In conclusion, we tackle the issue of highly unstable airframe aero-propulsion dynamics by using state-feedback LQR to guarantee stability of the nominal plant. However, LQR has no explicit means of dealing with the varying parameters and uncertainties. Therefore, we incorporate a H_∞ optimal controller for robust stability. The LQR controller is on the feedback loop providing disturbance rejection and stability with no increase in the number of closed-loop states and forms the inner loop of the overall control architecture.The H_∞ controller forms the outer loop and is on the forward path, for reference tracking. The H_∞ framework enables the designer to deal with uncertainties, making the overall two-loop hybrid controller a preferable choice to achieve robustness and stability.

REFERENCES

Anderson, B.D. and Moore, J.B. (1989). *Optimal Control: Linear Quadratic Control*.

Cimen, T. (2008). State-dependent riccati equation (SDRE) control: A survey. 3761–3775.

Doyle, J.C., Glover, K., Khargonekar, P.P., and Francis, B.A. (1989). State-space solutions to standard H2 and H-infinity control problems. *IEEE Transactions of Automatic Control*, 34(8), 831–847.

Glover, K. and Mcfarlane, D. (1989). Robust sabilization of normalised coprime factor plant descriptions with h inf bounded uncertainty.

Hyde, R.A. (1995). *H-infinity Aerospace Control Design - A VSTOL Flight application*.

Reichert, R. (1989). Application of H-infinity control to missile autopilot design.

Reichert, R. (1990). Robust autopilot design for aircraft with multiple lateral-axes controls using H-infinity synthesis.

S. Skogestad, M. Morari, J.D. (1988). Robust control of ill-conditioned plants: High-purity distillation. *IEEE Transactions on Automatic Control*, 33, 1092–1105.

Safonov, M.G. and Athans, M. (1976). Gain and phase margin for multiloop LQG regulators.

Skogestad, S. and Postlethwaite, I. (1996). *Multivariable Feedback Control: Analysis and design*.

Thompson, P. and Chiang, R. (1990). H-infinity robust control synthesis for a fighter performing a coordinated bank turn.

Urban, T., Iwaskiw, P., and Iglesias, P. (1999). Understanding missile autopilot using the H-infinity loop shaping design procedure.

Zames, G. (1981). Feedback and optimal sensitivity: Model reference transformations, multiplicative seminorms, and approximate inverses.

Zhou, K. and Doyle, J. (1998). *Essentials of Robust Control*.

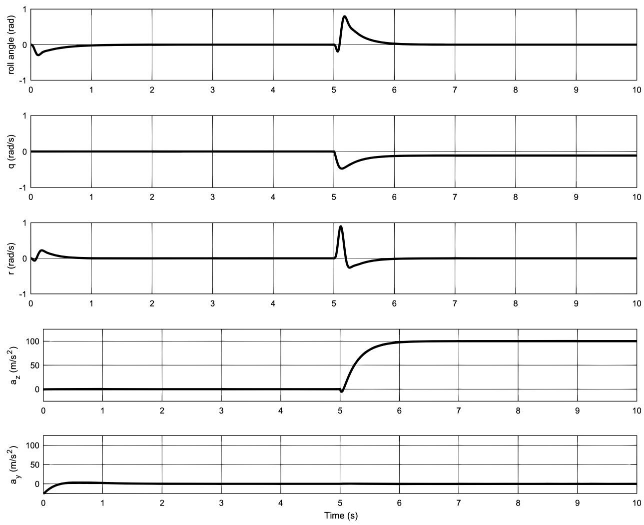

Fig. 6. Step Response to desired pitch acceleration command $A_{zd} = 100\, m/s^2$

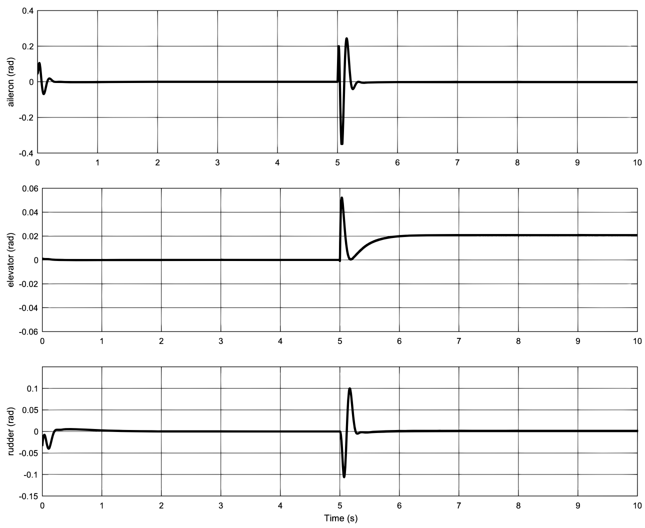

Fig. 7. Controller effort to desired pitch acceleration command $A_{zd} = 100\, m/s^2$

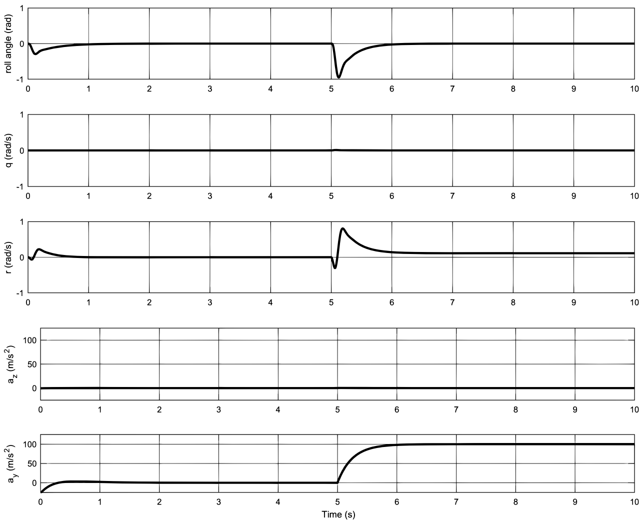

Fig. 8. Step Response to desired yaw acceleration command $A_{yd} = 100\ m/s^2$

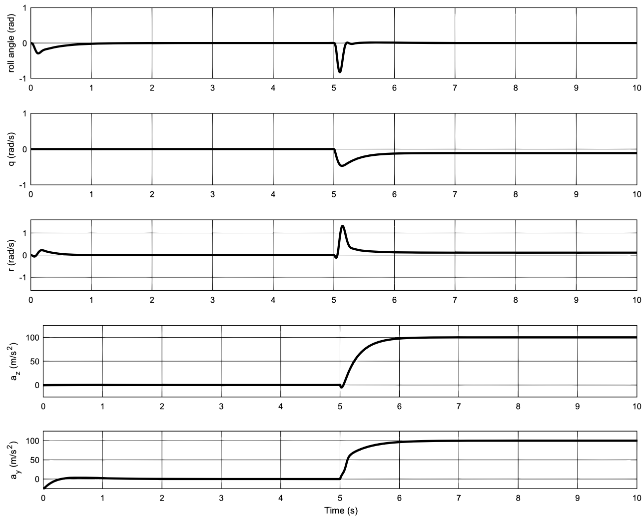

Fig. 10. Step Response to both desired pitch and yaw acceleration command $A_{zd} = A_{yd} = 100\ m/s^2$

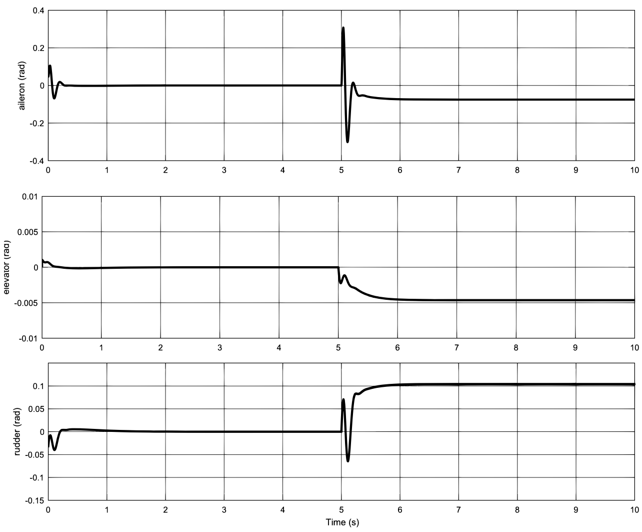

Fig. 9. Controller effort to desired yaw acceleration command $A_{yd} = 100\ m/s^2$

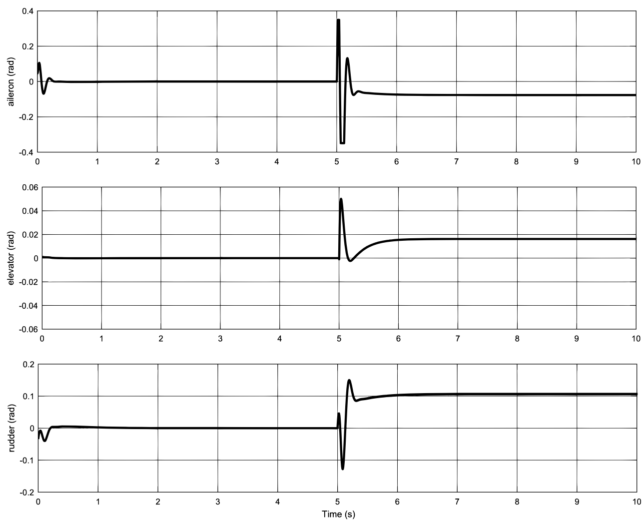

Fig. 11. Controller effort to both desired pitch and yaw acceleration command $A_{zd} = A_{yd} = 100\ m/s^2$